



Queensland University of Technology
Brisbane Australia

This is the author's version of a work that was submitted/accepted for publication in the following source:

Alonso-Caneiro, David, Shaw, Alyra J., & Collins, Michael J. (2012) Using optical coherence tomography to assess corneoscleral morphology after soft contact lens wear. *Optometry and Vision Science*, 89(11), pp. 1619-1626.

This file was downloaded from: <http://eprints.qut.edu.au/55078/>

© Copyright 2012 American Academy of Optometry

This is a non-final version of an article published in final form in *Optometry and Vision Science*, Volume 89(11), November 2012, p 1619–1626.

Notice: *Changes introduced as a result of publishing processes such as copy-editing and formatting may not be reflected in this document. For a definitive version of this work, please refer to the published source:*

<http://dx.doi.org/10.1097/OPX.0b013e31826c5f63>

Using OCT to assess corneoscleral morphology after soft contact lens wear

David Alonso-Caneiro, Ph.D., Alyra J. Shaw, Ph.D., Michael J. Collins, Ph.D.

Contact Lens and Visual Optics Laboratory,

School of Optometry and Vision Science,

Queensland University of Technology,

Australia

The manuscript contains 7 figures and no tables

Corresponding author:

David Alonso-Caneiro

School of Optometry and Vision Science, Queensland University of Technology,

Victoria Park Road, Kelvin Grove, Qld 4059, Australia

Phone: 07-3864 5716, Fax: 07-3864 5665

E-mail: d.alonsocaneiro@qut.edu.au

Financial interest of the authors: none

2 May, 2012

Purpose. To evaluate the use of optical coherence tomography (OCT) to assess the effect of different soft contact lenses on corneoscleral morphology.

Methods. Ten subjects had anterior segment OCT B-scans taken in the morning and again after six hours of soft contact lens wear. For each subject, three different contact lenses were used in the right eye on non-consecutive days, including a hydrogel sphere, a silicone hydrogel sphere and a silicone hydrogel toric. After image registration and layer segmentation, analyses were performed of the first hyper-reflective layer (HRL), the epithelial basement membrane (EBL) and the epithelial thickness (HRL to EBL). A root mean square difference (RMSD) of the layer profiles and the thickness change between the morning and afternoon measurements, was used to assess the effect of the contact lens on the corneoscleral morphology.

Results. The soft contact lenses had a statistically significant effect on the morphology of the anterior segment layers ($p < 0.001$). The average amounts of change for the three lenses (average RMSD values) for the corneal region were lower ($3.93 \pm 1.95 \mu\text{m}$ for the HRL and $4.02 \pm 2.14 \mu\text{m}$ for the EBL) than those measured in the limbal/scleral region ($11.24 \pm 6.21 \mu\text{m}$ for the HRL and $12.61 \pm 6.42 \mu\text{m}$ for the EBL). Similarly, averaged across the three lenses, the RMSD in epithelial thickness was lower in the cornea ($2.84 \pm 0.84 \mu\text{m}$) than the limbal/scleral ($5.47 \pm 1.71 \mu\text{m}$) region. Post-hoc analysis showed that ocular surface changes were significantly smaller with the silicone hydrogel sphere lens than both the silicone hydrogel toric ($p < 0.005$) and hydrogel sphere ($p < 0.02$) for the combined HRL and EBL data.

Conclusions. In this preliminary study, we have shown that soft contact lenses can produce small but significant changes in the morphology of the limbal/scleral region and that OCT technology is useful in assessing these changes. The clinical significance of these changes is yet to be determined.

Introduction

The biomechanical interaction between the contact lens and the ocular surface is an important factor in the safe and successful wear of contact lenses. The fitting characteristics of the lens can influence its comfort, the quality of vision and the health of the eye. A well-fitting contact lens creates even but minimal pressure on the cornea. On the other hand, a poorly-fitting contact lens may have negative consequences that in the short term may include discomfort,¹ reduced vision quality,¹ and physiological changes² that may alter the shape of the underlying cornea and lead to loss of surface epithelial cells through friction.² In more extreme cases, longer term, excessive pressure may lead to scarring of the cornea³ or increase the possible risk of secondary infections through surface trauma.⁴

Current clinical methods of evaluating a soft contact lens fit include the subjective observation of lens centration and movement using a slit lamp biomicroscope. Vital dyes are used to assess the ocular surface after contact lens wear. Staining of ocular tissues may indicate that a contact lens fitted poorly either on the central cornea or on the sclera due to the lens periphery or edge profile.²

The anterior corneal changes that occur with different types of contact lenses including polymethyl methacrylates,⁵ rigid gas permeable^{6,7} and soft contact lenses of various materials (hydrogels^{8,9} and silicone hydrogels¹⁰) and designs (spherical and toric¹¹) have been well documented. Quantitative assessment of the effect of the contact lens on corneal topography or pachymetry can be achieved after lens removal with instruments such as videokeratoscopes or Scheimpflug cameras.¹¹ These instruments measure the cornea to a diameter of about 8-11 mm but are unable to assess beyond this to the corneoscleral limbus or sclera, which is of interest in soft contact lens wear as the contact lens periphery and edge is in contact with this region.

Optical coherence tomography (OCT)¹² has become a fundamental clinical and research tool for imaging of the eye in the recent years.¹³ The ability of this technique to capture cross sectional (or volumetric) images of tissue with high axial resolution (down to 3 μm), together with high-speed acquisition rates, make it ideal for imaging the anterior segment of the human eye (i.e. cornea and contact lens).^{14, 15} However, the literature regarding the use of OCT technology to assess contact lenses is still limited. A recent manuscript,¹⁶ identified fourteen studies that have used OCT technology to investigate contact lenses. Most of these studies have concentrated on corneal swelling and epithelial changes due to contact lens wear either under closed-eye conditions,¹⁷ rigid contact lens wear¹⁸ or overnight orthokeratology lens wear.¹⁹ A few studies have imaged contact lenses in-situ, examining contact lens thickness,²⁰ gaps between the lens and ocular surface and contact lens edge profiles.²¹ A recent study has assessed the corneoscleral transition zone, reporting that contrary to usual depictions, the corneoscleral zone is often smooth and tangential and that its topography is important in soft contact lens fitting.²² However, to the best of our knowledge, no studies using OCT imaging techniques have focused on the effect that soft contact lenses have on the morphology of the outer peripheral cornea and beyond (corneoscleral junction and sclera).

In this study, we used OCT to assess the effect of three different soft contact lenses on the periphery of the cornea, corneoscleral limbus and sclera. The methodology and image processing techniques were developed in this project to optimise OCT image quality and to allow quantitative and accurate measurements of the effect of the contact lens on the ocular surface. We hope that this study will provide an improved understanding of the nature of the interaction between the contact lens and ocular surface for soft contact lenses with different design and material characteristics.

Materials and Methods

Clinical protocol

Ten young subjects aged from 26 to 36 years (mean age 31 ± 4 years) were recruited for the study. All subjects gave informed consent and the study was approved by the university research ethics committee. All subjects had good general and ocular health, including screening for any anterior eye conditions that may contraindicate contact lens wear. Only one of the ten subjects was a regular soft contact lens wearer, and this subject was instructed not to wear contact lenses for at least 24 hours prior to each measurement day. During the statistical analysis we examined the data for this particular subject in order to check for any bias in their results. The mean values did not differ substantially from the other subjects, so the subject was included in the cohort.

For this study, each subject wore 3 commercially available soft contact lenses from the same manufacturer (hydrogel sphere, silicone hydrogel sphere and silicone hydrogel toric) in the right eye. These contact lenses were chosen so that there were a combination of contact lens materials (hydrogel or silicone hydrogel) and designs (sphere or toric) so that these factors could be considered in the analysis. Different base curves were used when needed to ensure that all the contact lenses fit well for each subject. A back vertex power of -1.75 D was used for all the spherical contact lenses while the toric lens power was chosen to be close to the spherical equivalent, being $-1.00 / -1.75 \times 180$ for all the toric lenses.

The study was conducted over three non-consecutive days with each measurement day consisting of a morning measurement session (between 9 and 11 am), 6 hours of contact lens wear and then an afternoon measurement session (between 3 and 5 pm). In the morning, a baseline set of 5 mm horizontal B-scans were taken on both the nasal and temporal sides of the cornea (12 measurements in total), approximately centred at the limbal junction, using the

commercial high-resolution spectral-domain OCT (SOCT Copernicus HR, Optopol Technology SA, Zawiercie, Poland). After this, one of the three contact lenses was inserted into the right eye of the subject and the fit assessed after 10 minutes. Different base curves were used for different subjects to achieve acceptable fits, with the contact lenses being well centred, some movement with upgaze blinking and able to be easily moved with digital pressure (push-up test). After 6 hours, the contact lens was removed and another set of B-scans were immediately recorded. A slit lamp examination followed, including fluorescein instillation to record and photograph any changes due to the contact lens.

Methods for OCT data acquisition and analysis

The SOCT Copernicus HR is a spectral domain OCT instrument that provides high-resolution cross-sectional images of the posterior and anterior segments of the eye. The SOCT HR device uses a superluminescent diode light source with a wavelength of 840 nm, has an axial resolution of 3 μm and a scanning speed of 52,000 A-scans/s. A set of procedures during the data acquisition phase were followed in order to ensure a good image quality and repeatable measurements. For each subject, a 5 mm width scan using the instrument's *animation scanning mode* was acquired. The selected width is the instrument's maximum width for anterior segment imaging. This scanning mode allows the capture of multiple consecutive B-scans from the same location in a single acquisition. A total of 30 horizontal cross-sectional scans (with each of the 30 B-scans consisting of 1500 A-scans) were collected at each measurement in a total scan time of 1.14 s. Each of these measurements, which are formed by a set of consecutive B-scans, were aligned and averaged to reduce noise and improve the image contrast. This custom design image processing technique uses a hierarchical model-based motion (HMBM) estimation based on a rigid-motion model, which compensates for image translation and rotation. The details of this processing method have been presented elsewhere.²³ The final outcome of each *animation mode* measurement, is a single averaged

B-scan with reduced noise and subsequently with a clearer distinction between tissue layers. Figure 1 shows an example of one single B-scan out of the set [Figure 1(A)] and the aligned average of 30 B-scans for a representative subject [Figure 1(B)].

The OCT imaging instrument used in this study is limited by a maximum imaging depth of 2 mm (i.e. 2 mm depth in the cross-sectional image). Additionally, as the depth increases the contrast decreases. To obtain the best image quality, the subjects were instructed to keep their head straight while looking off-axis (25 degrees eye rotation). The fixation target was a cross placed at 25 degrees and 3 metres behind the subject and viewed using a mirror attached to the instrument (Figure 2 presents a schematic of this setup). This configuration ensured that the measurement region (i.e. anterior segment) was quasi-perpendicular to the instrument, thus the ocular surface had minimal depth, and therefore better contrast was achieved across the 5 mm horizontal scan.

The instrument has an *eye preview* camera to assist with the alignment of the subject. To further improve the *eye preview* image quality and enhance the iris features, external illumination was used. Before the commencement of the study each subject had a test measurement taken in order to determine the iris feature to be used for alignment during the study. The selected feature had to be located approximately at the 3 o'clock position for the nasal scan and at 9 o'clock for the temporal scan. Six measurements were taken per side (nasal and temporal) in each session (morning and afternoon). Figure 2 shows an example of two eye preview images in the morning and afternoon and its corresponding B-scan.

Following data collection, the best three measurements (for each measurement side and session) were manually chosen based on the *eye preview* images for further analysis. The three selected morning and afternoon measurements (6 in total per side) were realigned to a common axis to ensure that all 6 images had a common reference and could then be compared

for changes in morphology. Thus, any layer or thickness change observed between morning and afternoon measurements should be due to the effect of the contact lens and not to image or instrument misalignment. The realignment of the 6 images was automatically done using the same HMBM processing scheme.²³ Figure 3 shows an example of a morning (AM) and an afternoon (PM) measurement on the nasal side of a subject after wearing a silicone hydrogel toric lens for 6 hours. Both AM and PM images are aligned to a common reference location (centre column). Then in the right column of the figure shows the superimposed image that combines the aligned AM and PM images. In order to appreciate the details, a zoomed region of interest is provided below. In this example, an indentation in the scleral surface is clearly visible after wearing the silicone hydrogel toric contact lens.

The final analysis step was to manually segment the two tissue layers from each image: the first hyper-reflective layer (HRL) corresponding to the tear film overlying the anterior corneal surface and the second hyper-reflective layer at the epithelial basement membrane (EBL). The difference between these layers is most likely to represent the epithelial thickness of the cornea and conjunctiva overlying the sclera, plus the tear layer. If we infer a change in epithelial thickness or morphology associated with the experiment, we therefore have to assume that any change in tear layer thickness between measurements is negligible, or at least comparatively small compared with the tissue morphology change. Given the thickness of the tear film compared with the corneal tissues of interest, this would seem a reasonable assumption.

For the manual segmentation process, each image was vertically divided into three equal sections and presented to the operator. At least 10 points for each section were manually selected so that there were at least 30 points per layer, for each image. Then, the algorithm fits a smooth spline function between the points along the boundaries to define the layers. Thus, for each image, an HRL and EBL layer profile were obtained. The spline function has been

previously used to fit OCT retinal layers that have a complex shape and can not be properly fitted by a polynomial function.^{24, 25} The averages of these measurements (morning and afternoon) were used for further analyses.

To investigate the effect of the soft contact lens on eye in different regions, each scan was manually divided into corneal and limbal/scleral regions using the termination of Bowman's layer as the division point or corneolimbal junction (see Figure 4). In the subsequent analysis we adopt the terminology, *region* (corneal versus limbal) and *side* (nasal versus temporal) to describe the areas under investigation. Figure 4 presents the superimposed images (3xAM and 3xPM images) with the average HRL and EBL layers, before and after 6 hours of contact lens wear, and the division into regions is also shown.

In summary, to observe any lens effects in each of the regions, we investigated three major parameters, the change in the HRL profile, the change in the EBL profile and the epithelial thickness change between HRL-EBL. The change in any of these parameters (HRL, EBL and epithelial thickness) was assessed by calculating the root means square difference (RMSD) between the averaged pre- and post-contact lens wear profiles. This RMSD parameter basically provides an overall value related to the profile/thickness changes. The RMSD is a quadratic mean of the difference, so if the value is close to zero it means there was little difference in the profile or thickness of the layer between the morning and afternoon measurements (i.e. no lens effect). Repeated measures analysis of variance (ANOVA) was carried out with three within-subject factors (region, side and type of contact lens) to investigate for any significant changes in each of the layers or thicknesses, with post-hoc analysis completed for the contact lens factor.

Results

Layer profile changes

The group mean RMSD values for the HRL and EBL layers are shown in Figure 5. The RMSD values for both layers were highly correlated (Pearson's correlation, $r=0.94$). Each of the layer's profile (HRL and EBL) was found to exhibit a significant difference in RMSD value as a function of the region (i.e. corneal vs limbal/scleral) (repeated measures ANOVA, $p<0.001$). The average RMSD values for all three lens types in the corneal region were lower ($3.93\pm1.95\text{ }\mu\text{m}$ for the HRL and $4.02\pm2.14\text{ }\mu\text{m}$ for the EBL) than for the limbal/scleral region ($11.24\pm6.21\text{ }\mu\text{m}$ for the HRL and $12.61\pm6.42\text{ }\mu\text{m}$ for the EBL), indicating that a larger change in morphology occurred in the limbal/scleral region than in the corneal region.

There was no significant difference between the changes in the nasal and temporal sides of the HRL and EBL layers, so in the subsequent analyses we provide mean data for both sides (nasal and temporal) combined. The mean RMSD values in the limbal/scleral region were; for the silicone hydrogel toric ($11.70\pm4.44\text{ }\mu\text{m}$ for the HRL and 12.29 ± 4.84 for the EBL), for the silicone hydrogel sphere ($8.55\pm4.60\text{ }\mu\text{m}$ for the HRL and $9.60\pm5.32\text{ }\mu\text{m}$ for the EBL) and for the hydrogel sphere ($11.77\pm8.48\text{ }\mu\text{m}$ for the HRL and $13.58\pm8.24\text{ }\mu\text{m}$ for the EBL).

There was a significant difference between the contact lenses in their effects on the morphology (repeated measures ANOVA, $p=0.03$). Post-hoc analysis showed that ocular surface changes were significantly smaller with the silicone hydrogel sphere lens than both the silicone hydrogel toric ($p<0.005$) and hydrogel sphere ($p<0.02$) for the combined HRL and EBL data.

Epithelial thickness changes

The group mean RMSD of epithelial thickness is presented in Figure 5. There was a significant difference in the RMSD epithelial thickness change as a function of the region (corneal vs limbal/scleral) measured (repeated measures ANOVA, $p < 0.001$), with a 2.84 ± 0.84 μm mean RMSD epithelial thickness change in the corneal region and a larger change of 5.47 ± 1.71 μm mean RMSD in the limbal/scleral region. The interaction between RMSD epithelial change and contact lens type showed no statistical significance ($p > 0.05$). Similarly, there was no statistically significant difference ($p > 0.05$) found between sides (nasal vs temporal).

The group mean change in epithelial thickness (HRL to EBL) on the corneal side of the limbus showed an overall thinning of 0.50 ± 1.61 μm , while the limbal/scleral region also showed thinning of 0.97 ± 2.74 μm . No statistically significant difference was found in the amount of thinning in these regions (corneal vs. limbal/scleral) ($p > 0.05$).

Discussion

We found that all of the soft contact lenses caused subtle, but statistically significant changes in the anterior segment layers (HRL and EBL), and that the changes were greatest in the limbal/scleral region. This regional difference coincides with the contact zone of the edge of the soft lens on the ocular surface and presumably results from greater pressure in this region. The topography of the limbus and sclera is not well defined, however it is generally thought to have a flatter radius of curvature than the central and peripheral cornea in most meridians.^{2,}

²² Depending upon factors such as the design of the back surface of the contact lens and its biomechanical wrapping properties, the edge of a soft lens is likely to exert pressure on the

ocular surface. So called “limbal indentation” is a well known clinical manifestation of a tight fitting soft contact lens,² however the soft lens fits in our study would not be classified as tight. Normal soft lens movement associated blinking and eye excursions are also likely to cause some pressure and friction between the edge of the soft lens and the surface of the eye, if the shape of the sclera is progressively flattening away from the limbus. This pressure and friction at the edge of the lens, in combination with the edge design, is possibly a contributing cause to the staining that is often seen after soft lens removal.^{2, 26} The mechanical force of soft contact lenses is also known to cause other changes to the ocular surface including conjunctival epithelial flaps²⁷ and conjunctival folds.²⁸

Interestingly mini-scleral rigid contact lenses, which typically vault the cornea, also create bearing on the sclera just past the limbus. These lenses have been reported to depress the conjunctiva over time when settling on the eye.²⁹ It is unknown which tissue layer is compressing, however it does suggest that the ocular surface past the limbus does change in response to contact lens pressure.

The periphery and edge of the three contact lenses used in the study are evident in Figure 6, which shows an example of B-scans for each of the three different contact lenses for the temporal side of the same subject. The silicone hydrogel toric lens has thickened stabilization zones towards the periphery along the horizontal meridian of the lens, that are likely to have been a major factor leading to greater pressure transmitted through the lens to the ocular surface in this region, compared with the spherical lenses. In a study of corneal topography changes associated with the wear of cosmetic tinted soft contact lenses, it was shown that heavily pigmented cosmetic soft lenses caused significant topography changes specifically at the junction (zone of greatest thickness difference) between the pigmented and clear regions in the centre of the soft lens.³⁰

There was no obvious thickening of the epithelium related to oedema under the thicker lens peripheral stabilization zones of the soft toric silicone hydrogel contact lenses, or the spherical silicone hydrogel or hydrogel lenses that could account for increased susceptibility to pressure at the lens edge.¹¹ The epithelium typically showed a small degrees of thinning after 6 hours lens wear in this study (less than 1 μm). However, for long-term contact lens wearers there is consistent evidence of greater thinning of the bulbar conjunctival epithelium³¹ and the overall corneal epithelium³² in previous studies using laser scanning confocal microscopy³¹ and optical pachymetry.³² Another factor that may influence the changes in morphometry is the inter-subject variations in limbus shape, in particular the angle of the corneoscleral junction. This factor, which now can be assessed with OCT instruments, has been shown to be of value in predicting contact lens fit.²² Although nasal and temporal limbal shapes are known to differ,²² our data showed no statistical difference between the effects of the contact lenses on the ocular surface on the nasal versus temporal sides of the eye.

In the current study, additional OCT images of the contact lens on eye were acquired 10 minutes after lens insertion and prior to lens removal. However since the eye was turned during the measurement, the natural contact lens position may have altered, and these images were not used in the analysis. Despite this, it was interesting to notice the potential of the OCT to assess the fit of the lens and to evaluate the relationship between the ocular surface and the contact lens over time. As an example, Figure 7 shows a morning and afternoon measurement for the silicone hydrogel toric lens, on the same subject. The afternoon measurement shows a gap between the lens back surface at the limbus that was not be observed in the morning measurement. Similar observations were made for other subjects while wearing the soft toric design. These gaps have also been reported recently using OCT imaging for different lens designs and illustrate imperfect wrapping of the lens to the ocular surface,²¹ the cause of which is not yet established.

The methodology and image processing techniques were developed in this project to optimise OCT image quality, as well as to allow quantitative measurements of the effect of the contact lens on the ocular surface. We have demonstrated that OCT technology can be used to assess the effect of the contact lenses on the morphology of the corneoscleral region. Despite the relatively small sample size of this preliminary study, we were able to observe statistically significant differences in the effect of soft contact lens wear on the corneoscleral morphology. The association between the changes we found in the morphology of the corneoscleral surface layers and other clinical findings is yet to be determined.

Acknowledgments

The authors thank Brett Davis for his assistance with the experimental set-up of the study. Some aspects of this study were presented at the 2012 Association for Research in Vision and Ophthalmology (ARVO) annual meeting.

References

1. Dumbleton KA, Chalmers RL, McNally J, Bayer S, Fonn D. Effect of lens base curve on subjective comfort and assessment of fit with silicone hydrogel continuous wear contact lenses. *Optom Vis Sci* 2002;79:633-7.
2. Young G, Coleman S. Poorly fitting soft lenses affect ocular integrity. *Eye Contact Lens* 2001;27:68-74.
3. Korb DR, Finnemore VM, Herman JP. Apical changes and scarring in keratoconus as related to contact lens fitting techniques. *J Am Optom Assoc* 1982;53:199-205.
4. Stapleton F, Keay L, Edwards K, Naduvilath T, Dart JKG, Brian G, Holden BA. The incidence of contact lens-related microbial keratitis in Australia. *Ophthalmology* 2008;115:1655-62.
5. Wilson SE, Lin DT, Klyce SD, Reidy JJ, Insler MS. Topographic changes in contact lens-induced corneal warpage. *Ophthalmology* 1990;97:734-44.
6. Schwallie JD, Barr JT, Carney LG. The effects of spherical and aspheric rigid gas permeable contact lenses: corneal curvature and topography changes. *International Contact Lens Clinic* 1995;22:67-79.
7. Yebra-Pimentel E, Giraldez MJ, Arias FL, Gonzalez J, Gonzalez JM, Parafita MA, Febrero M. Rigid gas permeable contact lens and corneal topography. *Ophthalmic Physiol Opt* 2001;21:236-42.
8. Arranz I, Gonzalez-Garcia MJ, Galarreta DJ, Cisneros AB, Calonge M, Herreras JM. Low water content hydrogel contact lenses (HCL) induce corneal irregularity. *Invest Ophthalmol Vis Sci* 2003;44:3701.
9. Schornack M. Hydrogel contact lens-induced corneal warpage. *Cont Lens Anterior Eye* 2003;26:153-9.
10. Alba-Bueno F, Beltran-Masgoret A, Sanjuan C, Biarnas M, Maran J. Corneal shape changes induced by first and second generation silicone hydrogel contact lenses in daily wear. *Cont Lens Anterior Eye* 2009;32:88-92.
11. Tyagi G, Collins M, Read S, Davis B. Regional changes in corneal thickness and shape with soft contact lenses. *Optom Vis Sci* 2010;87:567-75.
12. Huang D, Swanson EA, Lin CP, Schuman JS, Stinson WG, Chang W, Hee MR, Flotte T, Gregory K, Puliafito CA. Optical coherence tomography. *Science* 1991;254:1178-81.
13. Wojtkowski M. High-speed optical coherence tomography: basics and applications. *Appl Opt* 2010;49:D30-D61.
14. Grulkowski I, Gora M, Szkulmowski M, Gorczynska I, Szlag D, Marcos S, Kowalczyk A, Wojtkowski M. Anterior segment imaging with Spectral OCT system using a high-speed CMOS camera. *Opt Express* 2009;17:4842-58.
15. Gora M, Karnowski K, Szkulmowski M, Kaluzny BJ, Huber R, Kowalczyk A, Wojtkowski M. Ultra high-speed swept source OCT imaging of the anterior segment of human eye at 200 kHz with adjustable imaging range. *Opt Express* 2009;17:14880-94.
16. Gonzalez-Meijome JM, Cerviño A, Carracedo G, Queiros A, Garcia-Lázaro S, Ferrer-Blasco T. High-Resolution Spectral Domain Optical Coherence Tomography Technology for the Visualization of Contact Lens to Cornea Relationships. *Cornea* 2009;29:1359-67.
17. Wang J, Fonn D, Simpson TL, Jones L. The measurement of corneal epithelial thickness in response to hypoxia using optical coherence tomography1. *Am J Ophthalmol* 2002;133:315-9.

18. Haque S, Fonn D, Simpson T, Jones L. Corneal refractive therapy with different lens materials, part 1: corneal, stromal, and epithelial thickness changes. *Optom Vis Sci* 2007;84:343-8.
19. Haque S, Fonn D, Simpson T, Jones L. Corneal and epithelial thickness changes after 4 weeks of overnight corneal refractive therapy lens wear, measured with optical coherence tomography. *Eye Contact Lens* 2004;30:189-93.
20. Gonzalez-Meijome JM, Cerviño A, Peixoto-de-Matos SC, Madrid-Costa D, Jorge J, Ferrer-Blasco T. " In Situ" Corneal and Contact Lens Thickness Changes With High-Resolution Optical Coherence Tomography. *Cornea* 2012;31:633-8.
21. Shen M, Cui L, Riley C, Wang MR, Wang J. Characterization of soft contact lens edge fitting using ultra-high resolution and ultra-long scan depth optical coherence tomography. *Invest Ophthalmol Vis Sci* 2010;52:4091-7.
22. Hall LA, Young G, Wolffsohn JS, Riley C. The Influence of Corneoscleral Topography on Soft Contact Lens Fit. *Invest Ophthalmol Vis Sci* 2011;52:6801-6.
23. Alonso-Caneiro D, Read SA, Collins MJ. Speckle reduction in optical coherence tomography imaging by affine-motion image registration. *J Biomed Opt* 2011;16:116027.
24. Hood DC, Cho J, Raza AS, Dale EA, Wang M. Reliability of a computer-aided manual procedure for segmenting optical coherence tomography scans. *Optom Vis Sci* 2011;88:113-23.
25. Read SA, Collins MJ, Alonso-Caneiro D. Diurnal variation of retinal thickness with spectral domain OCT. *Optom Vis Sci* 2012;89:611-9.
26. Maissa C, Guillon M, Garofalo RJ. Contact Lens-Induced Circumlimbal Staining in Silicone Hydrogel Contact Lenses Worn on a Daily Wear Basis. *Eye Contact Lens* 2012;38:16-26.
27. Bergmanson JPG, Tukler J, Leach NE, Alabdelmoneam M, Miller WL. Morphology of contact lens-induced conjunctival epithelial flaps: A pilot study. *Cont Lens Anterior Eye* 2012;(in press).
28. Tapasztó B, Veres A, Kosina-Hagyó K, Somfai GM, Németh J. OCT Imaging of Lid-Parallel Conjunctival Folds in Soft Contact Lens Wearers. *Optom Vis Sci* 2011;88:1206-13.
29. van der Worp E. A Guide to Scleral Lens Fitting [monograph online]. Scleral Lens Education Society 2010;Available at: <http://commons.pacificu.edu/mono/4/> Accessed June 21, 2012:1-64.
30. Voetz SC, Collins MJ, Lingelbach B. Recovery of corneal topography and vision following opaque-tinted contact lens wear. *Eye Contact Lens* 2004;30:111-7.
31. Efron N, Al-Dossari M, Pritchard N. Confocal microscopy of the bulbar conjunctiva in contact lens wear. *Cornea* 2010;29:43-52.
32. Perez JG, G. MJM, Jalbert I, Sweeney DF, Erickson P. Corneal epithelial thinning profile induced by long-term wear of hydrogel lenses. *Cornea* 2003;22:304-7.

Figures

Figure 1. B-scan images of the anterior segment showing the cornea, the corneoscleral junction and the sclera. (A) Single B-scan and (B) B-scan after HMBM speckle reduction. Note the enhanced definition of the corneoscleral features in the speckle-reduced image, the inset provides a zoomed region of interest in the cornea.

Figure 2. The experimental set-up (left column) ensured repeatable scans and optimal image quality with the subject keeping their head straight, while looking off-axis 25° to a fixation target. The centre column shows morning (AM) and afternoon (PM) *eye preview* images that were utilized in the subject's alignment. Iris features located approximately at the 3 o'clock position for the nasal scan (see arrows in the centre column) and at 9 o'clock for the temporal scan were used to align the scan. The corresponding B-scans are shown in the right column.

Figure 3. Example of image data set from the nasal side of a subject before lens insertion (AM) and after wearing a silicone hydrogel toric lens for 6 hours (PM) (left column). The AM and PM images are aligned to have a common reference (centre column). The images in the right column show the superposition of morning and afternoon measurements after alignment, as well as a zoomed region of interest.

Figure 4. Silicone hydrogel toric lens on eye (A). Superposition of all the images (3 morning and 3 afternoon) after alignment (B). The HRL and EBL are marked with grey dashed line for morning measurement and with a white solid line for the afternoon.

Figure 5. Box plot of group mean, root mean square difference (RMSD) for all subjects ($n=10$) for the different lenses, sides (nasal vs. temporal) and regions (cornea vs. limbal/scleral). The top plot corresponds to the first hyper-reflective layer (HRL), the middle

plot corresponds to the epithelial basement membrane (EBL) and the bottom plot corresponds to the epithelial thickness. The asterisks represent potential outliers in the data that were not excluded from the statistical analysis.

Figure. 6 Three B-scan measurements with each lens on eye: silicone hydrogel toric, silicone hydrogel sphere and hydrogel sphere. All the measurements correspond to the same subject and the measurements were taken in the morning on the temporal side. Similar features in the tissues can be observed for each image.

Figure 7. Example of a silicone toric lens on eye 10 minutes after insertion (A) and after 6 hours of contact lens wear (B) with a conjunctiva gap evident (white box). The inset provides a zoomed region of interest of the gap between the back surface of the contact lens and the conjunctiva.

Figures

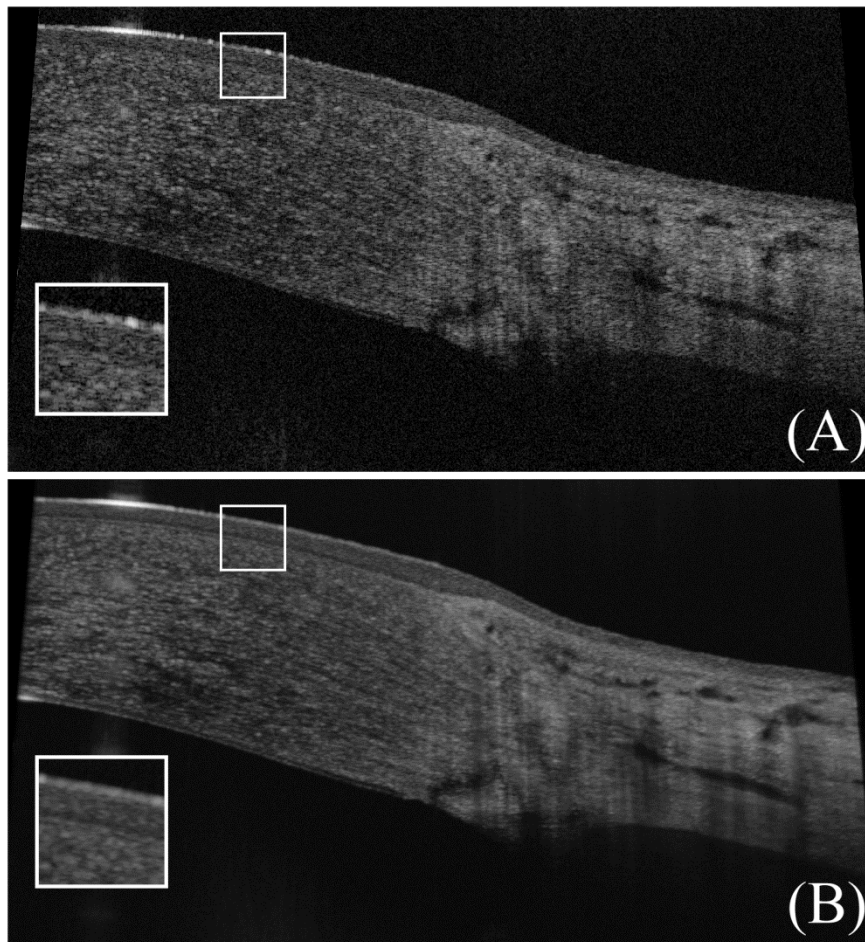


Figure 1. B-scan images of the anterior segment showing the cornea, the corneoscleral junction and the sclera. (A) Single B-scan and (B) B-scan after HMBM speckle reduction. Note the enhanced definition of the corneoscleral features in the speckle-reduced image, the inset provides a zoomed region of interest in the cornea.

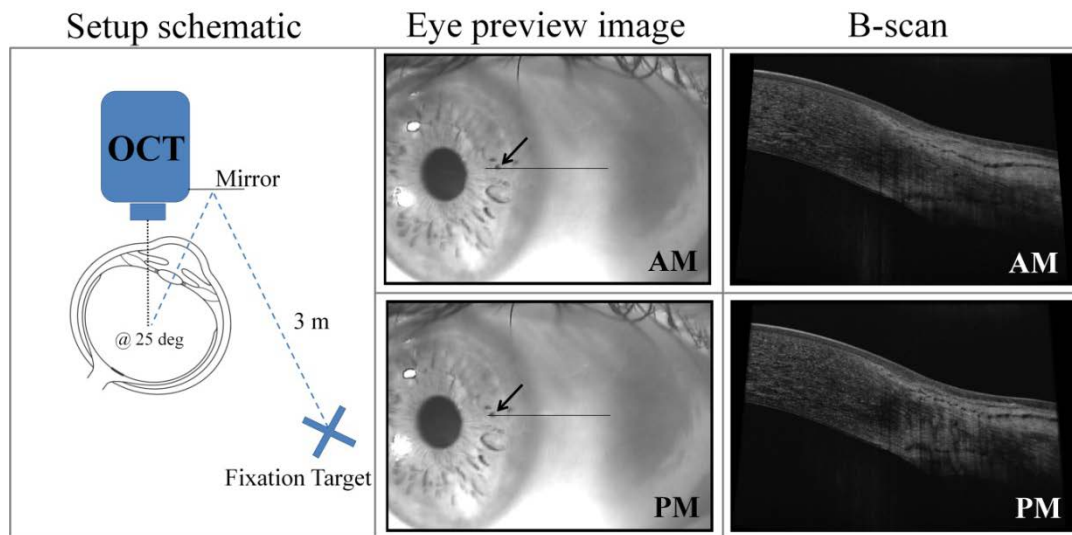


Figure 2. The experimental set-up (left column) ensured repeatable scans and optimal image quality with the subject keeping their head straight, while looking off-axis 25° to a fixation target. The centre column shows morning (AM) and afternoon (PM) *eye preview* images that were utilized in the subject's alignment. Iris features located approximately at the 3 o'clock position for the nasal scan (see arrows in the centre column) and at 9 o'clock for the temporal scan were used to align the scan. The corresponding B-scans are shown in the right column.

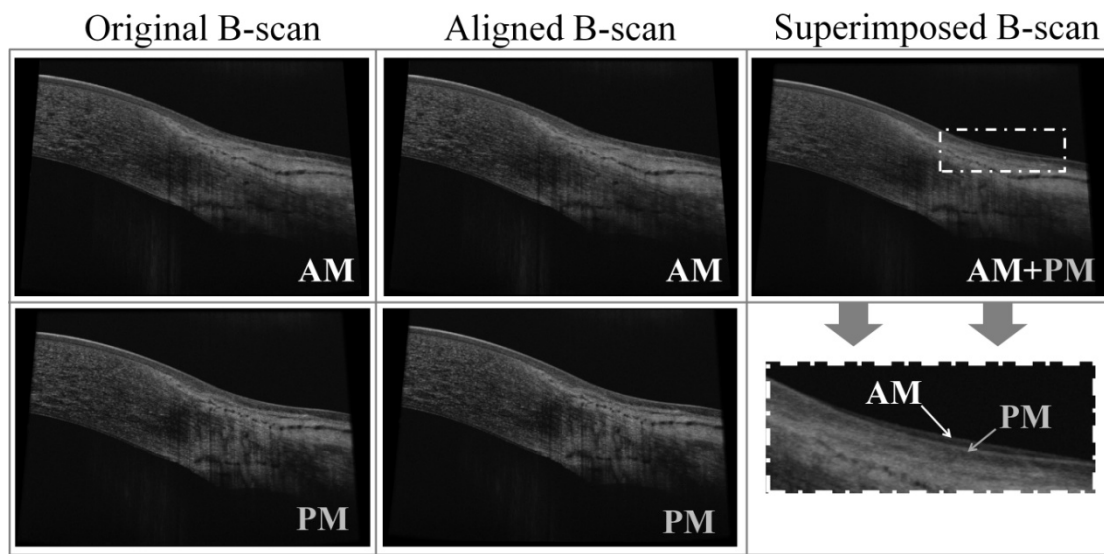


Figure 3. Example of image data set from the nasal side of a subject before lens insertion (AM) and after wearing a silicone hydrogel toric lens for 6 hours (PM) (left column). The AM and PM images are aligned to have a common reference (centre column). The images in the right column show the superposition of morning and afternoon measurements after alignment, as well as a zoomed region of interest.

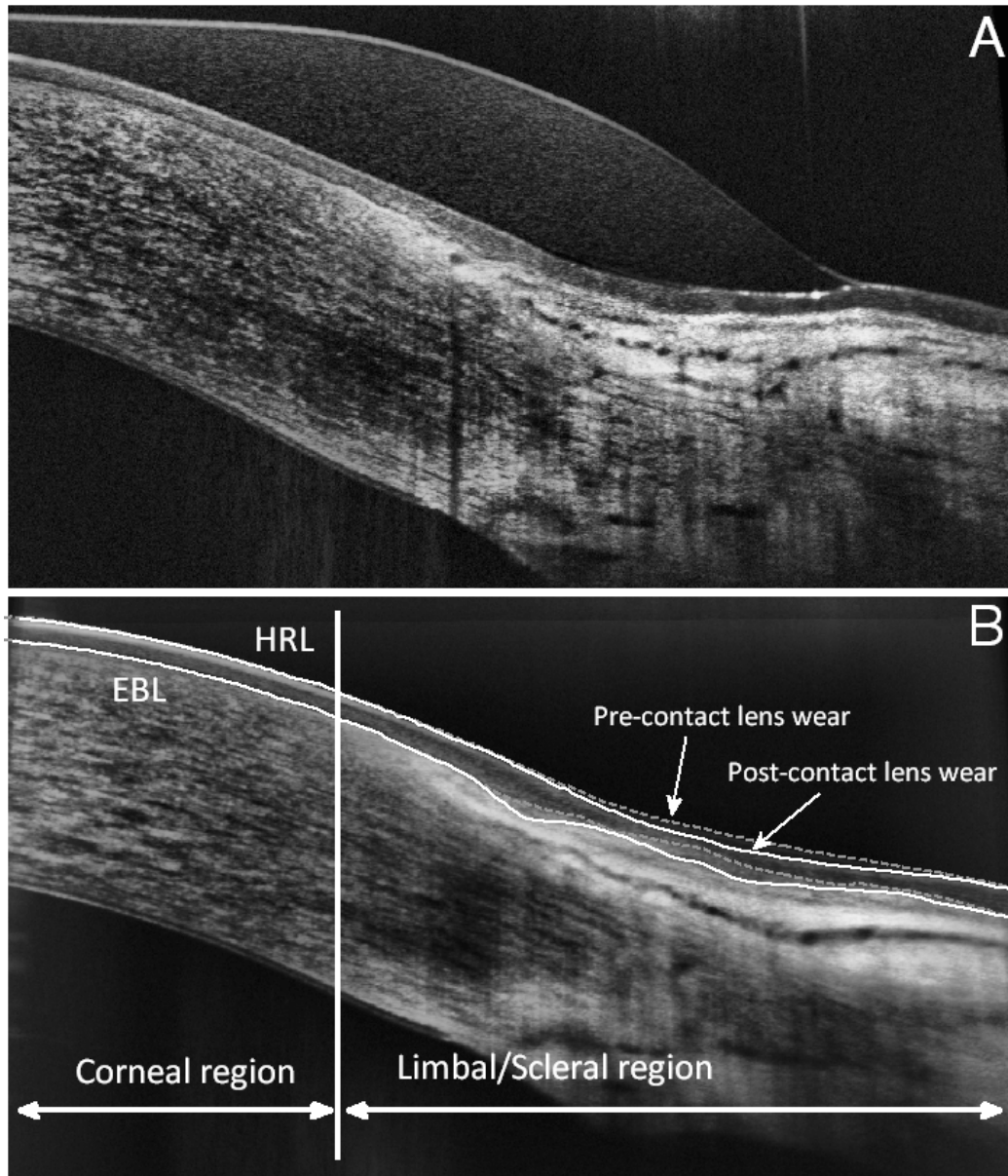


Figure 4. Silicone hydrogel toric lens on eye (A). Superposition of all the images (3 morning and 3 afternoon) after alignment (B). The HRL and EBL are marked with grey dashed line for morning measurement and with a white solid line for the afternoon.

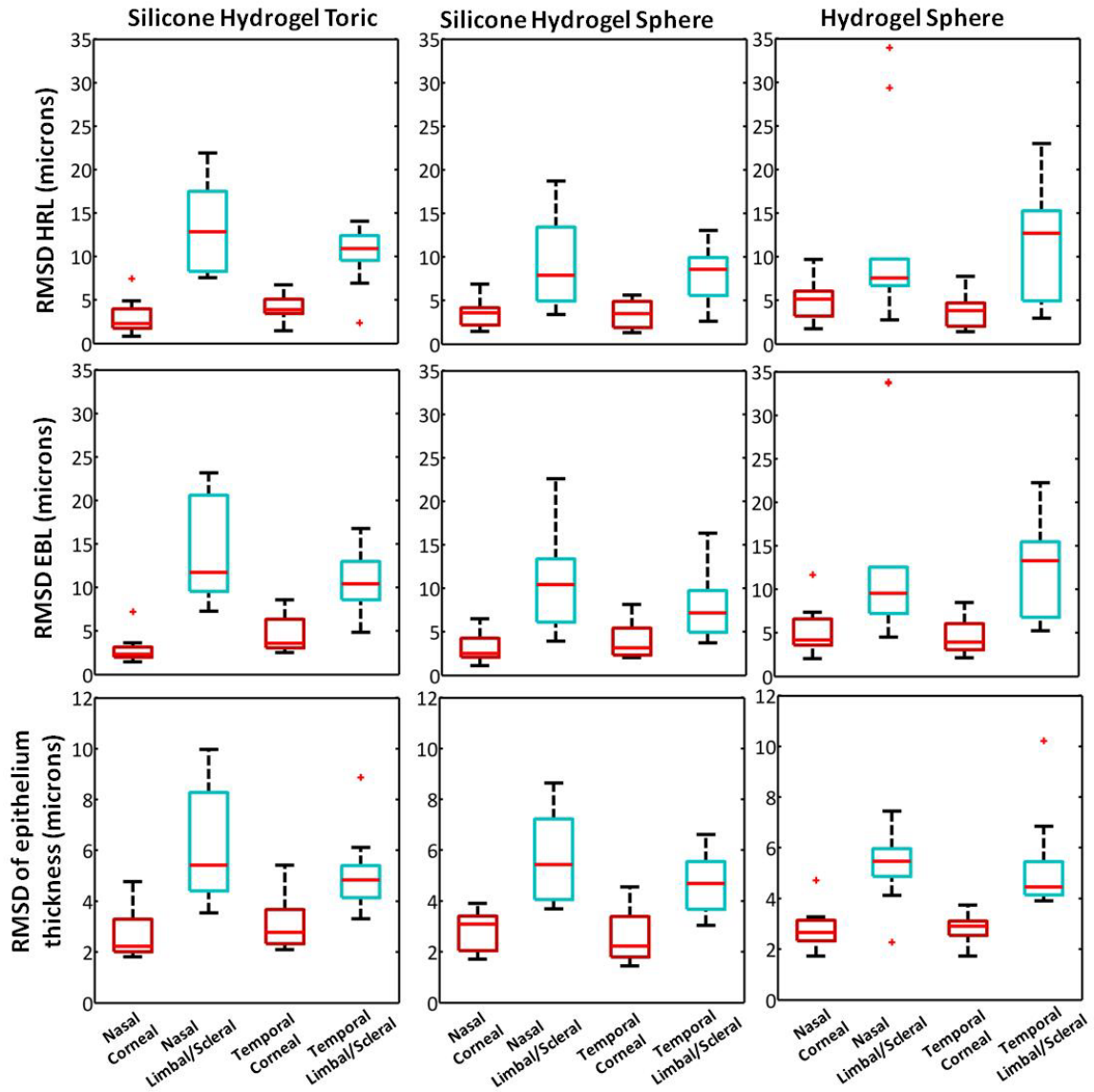


Figure 5. Box plot of group mean, root mean square difference (RMSD) for all subjects (n=10) for the different lenses, sides (nasal vs. temporal) and regions (cornea vs. limbal/scleral). The top plot corresponds to the first hyper-reflective layer (HRL), the middle plot corresponds to the epithelial basement membrane (EBL) and the bottom plot corresponds to the epithelial thickness. The asterisks represent potential outliers in the data that were not excluded from the statistical analysis.

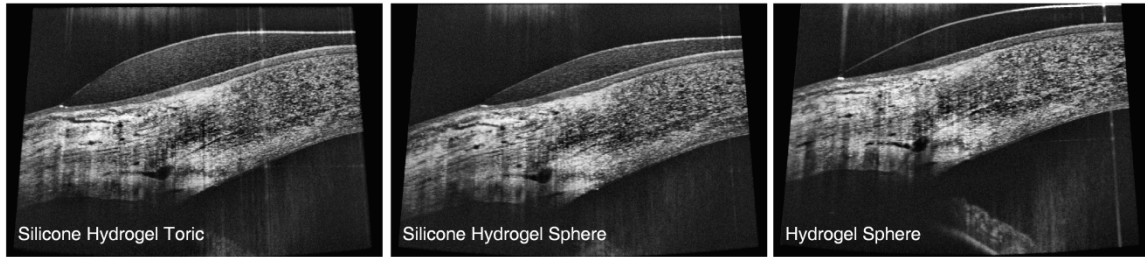


Figure. 6 Three B-scan measurements with each lens on eye: silicone hydrogel toric, silicone hydrogel sphere and hydrogel sphere. All the measurements correspond to the same subject and the measurements were taken in the morning on the temporal side. Similar features in the tissues can be observed for each image.

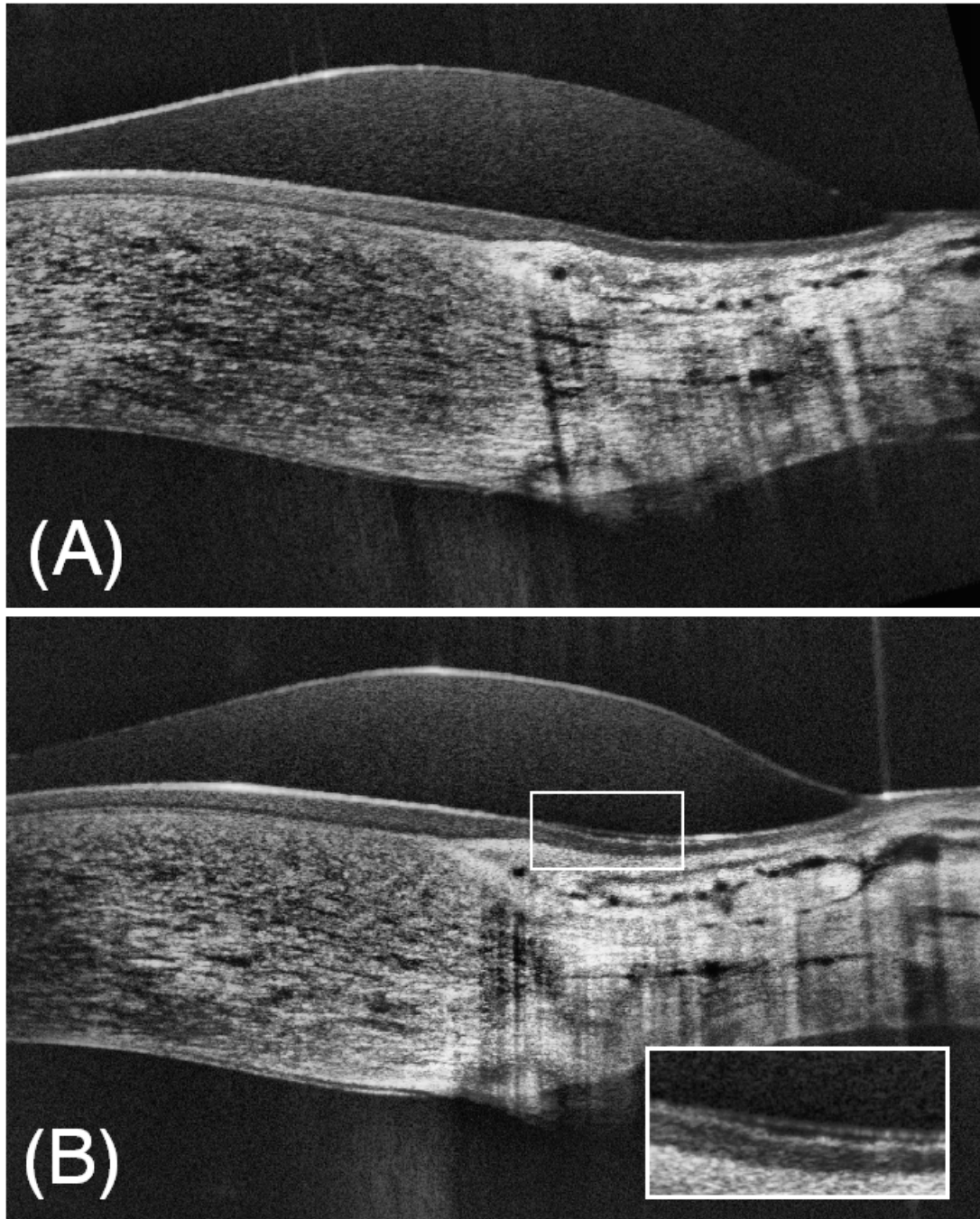


Figure 7. Example of a silicone toric lens on eye 10 minutes after insertion (A) and after 6 hours of contact lens wear (B) with a conjunctiva gap evident (white box). The inset provides a zoomed region of interest of the gap between the back surface of the contact lens and the conjunctiva.